# MACHINE LEARNING METHOD FOR IDENTIFICATION OF DISEASE FROM HUMAN AURA IMAGES

**Sarika G[1*], Dr. S. Palanikumar[2]**

**Abstract**

The human body is composed of energy that vibrates at various rates. Vibrant energy generates this magnetic field. All of our bodily functions, such as respiration, digestion, neurological and circulatory systems, and so on, are comprised of a series of electrochemical reactions. A combination of magnetic and electrical energy fields produces the "Bio-Energetic Field." The research in this area serves to bring to light a variety of intriguing concerns and traits which may be utilised to further the research work in this area on individuals based on human bio-field. The research in this area offers to learn more about the individual's mental state, health concerns, and other associated aspects. In order to better comprehend and interpret the human bio-field and highlight human existence, several improvements in this regard have been made. In the suggested process, we use AURA images to identify the changes. The Gas Discharge Visualisation (GDV) images is first preprocessed, then features are extracted, trained, and classified using machine learning techniques including Support Vector Machine, Random Forest (RF), and Ensembled AdaBoost (Eada). With the Ensembled AdaBoost technique, classification accuracy is increased on average.

***Keywords:-****Bio-field, Aura, GDV images, Machine Learning Techniques, Colour Co-occurrence Matrix*

[1*]Research Scholar Electronics and Communication Engineering Department Noorul Islam College for Higher Education Thukalay Email:- saranamith@gmail.com

[2]Former Associate Professor Information and Technology Department Noorul Islam College for Higher Education Thukalay Email:-palanikumarcsc@yahoo.com

***Corresponding Author**:- Sarika Amith

[*]Research Scholar Electronics and Communication Engineering Department Noorul Islam College for Higher Education Thukalay Email:- saranamith@gmail.com

**DOI: - 10.48047/ecb/2023.12.7.312**

## I. Introduction

Low-level heat, light, and sound energy with electrical and magnetic characteristics are emitted by the human body. Energy that chemistry and physics are unable to precisely describe may also be transported or converted. The human energy field, also known as the biologic field or biofield, is made up of all of these emissions. This human biofield holds distinctive data that can be used to predict and diagnose illnesses. The most recent advancements in biofield measurement are intended for medical research. Measurements are made of the many components of the biofield in order to identify organ and tissue dysfunctions before illnesses or symptoms manifest so that they can be effectively treated [1]. The "Bio-Energetic Field [2]" is produced by the interaction of the magnetic and electrical energy fields. The "Aura" is the name for the bio-energetic field that surrounds the human body and spans a space of

around 4 to 5 feet [3]. The fundamental hues of an aura resemble those of a rainbow. A person's mental and physical health has an impact on the colour and size of their aura. Chakras are energy concentration centres that exist within the human body. Figure 1 depicts the 122 minor and 7 main chakras in our body. The aura that surrounds our bodies is affected by any interference with the Meridian System and Chakras' regular operation.

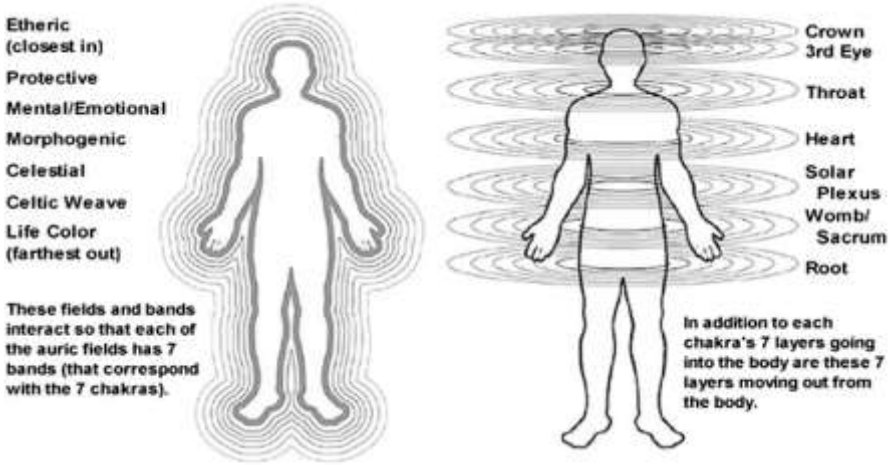


**Figure 1:** Chakra locations and the body's aura [4]

The visible and ultraviolet spectrums of ionising radiation are also produced by the human body. High-intensity radiation, such as infrared radiation, is emitted by the human body in certain spectral bands. The body emits a few hundred photons per second per square centimetre of surface area of low-intensity visible spectrum light. By emitting extremely low-level visible light, organisms referred to as "biophotons" may be able to convey vital electromagnetic bioinformation about the body. The first International Conference on Medical Biometrics was conducted in Hong Kong in 2008, and it promoted the notion that medical biometrics is a rapidly evolving, very promising, and trustworthy approach of automated medical diagnostics [5]. It differs from biometrics, a statistical method used in clinical practise, since it incorporates transdisciplinary technologies from biology, medicine, electronics, computers, and statistics.

Medical biometric systems have been created to solve health concerns and provide high-performance medical services. These systems use human traits in different media, such as photographs, signals, and other sources. There are several techniques that have been developed to assess the electromagnetic properties of the biofield. Due to the demand for automated disease detection, medical biometrics are a hot topic in our culture right now. Not all biometric tools deliver results instantly. Utilising the GDV device, an Electrophoton Capture (EPC) measurement that theorises measures the biophoton emissions from a person's aura, this study was created to assess the disease progression in a healthy population [6-8]. A prospective computerised biophysical screening of a person's psychophysiologic condition is offered by the GDV gadget [9]. Medical biometrics based on the GDV approach have been utilised to track patients and compare their electro-photonic emission naturally occurring before and after procedures, cancer treatments, energy healing, physiotherapy, SOQI therapy, and other medical procedures. prior research employing It may be able to spot deviations from normal functional status early in the course of a disease's development and keep track of the process of returning to normal functionality [9]. GDV's goal is to determine a person's functioning psychoemotional and physiological status by utilising their fingers [10]. The GDV biometric approach, in contrast to other biometrics, focuses on the extraction of biological patterns for health security.

The most popular technique for texture analysis is the Grey Level Co-occurrence Matrix (GLCM) approach. The link between colour information and gray-GLCM textural properties, however, is not well understood [11]. Furthermore, gray-GLCM textural features frequently exhibit global adaptability but lack local optimisation. Shearer [12] proposed using colour texture analysis in contrast to typical grey-level texture analysis to address these issues. Commonly used colour spaces including RGB, HSL, HSV, and L*a*b* have been utilised in image processing for processing agricultural products often [13]. The

HSL, HSV, and L*a*b* colour spaces were created to mimic how people see colour. The Colour Co-occurrence Matrix (CCM) approach for colour texture analysis is based on the idea that utilising visible-spectrum colour information gives images more characteristics than the conventional grey-level representation. The advantages of utilising texture analysis for biosensing approaches have been demonstrated in several research [14–19].

According to recent research by Shulginov. A. and Stadnik. O. S. [20], the significance attached to these hand-drawn and painted images and their historical history. Authors created and used an algorithm utilising an image processing approach to demonstrate science. According to their research, the aura image consists of colour, form, and contour. Then used the HSV colour space to describe the aura's colour space, and then used a histogram derivative of the intensity of the aura's outline to determine its form. Gunjan et al. [21] looked at the importance of human biofield data in prospective medical diagnosis. To design and construct an algorithm for the viewing and interpretation of the incredibly complex and dynamic aura colour patterns that surround a person, authors employed image processing and artificial intelligence approaches. They took a photo of the subject using a digital camera, and then they employed pre-processing methods to remove the noise. They applied image enhancement and normalisation, modifying the image's brightness and contrast, to improve the image's quality. After transforming the RGB image to a grayscale one, they utilised a machine learning method to identify the chakras in the image and created a new colour space to depict the subject's aura pattern. This new colour space is mapped using the RGB colour model, and the colour value is calculated using machine learning methods. Finally, using linear regression, a predicted report was created, detailing the effect of colours on the organs related to each chakra.

This study suggested using GDV images to recognise the medical condition. Image descriptors can help images convey more information. These intricate auras are used to extract features. These images are suitably classed based on them. SVM, RF, and Eada technique are used to study training and classification. In this research, preliminary work on GDV images for the body's illness detection is carried out. The remainder of this essay is structured as follows. The methodology for the proposed work is presented in Section II, the findings of the system are described in Section III, and the conclusions and future work of the research are presented in Section IV.

## II. Methodology

The suggested procedure comprised processes including pre-processing, feature extraction, and classification. Figure 2 displays the proposed structure's general block diagram. Pre-processing is necessary for feature extraction in order to deal with the images' noise reduction and contrast adjustments.

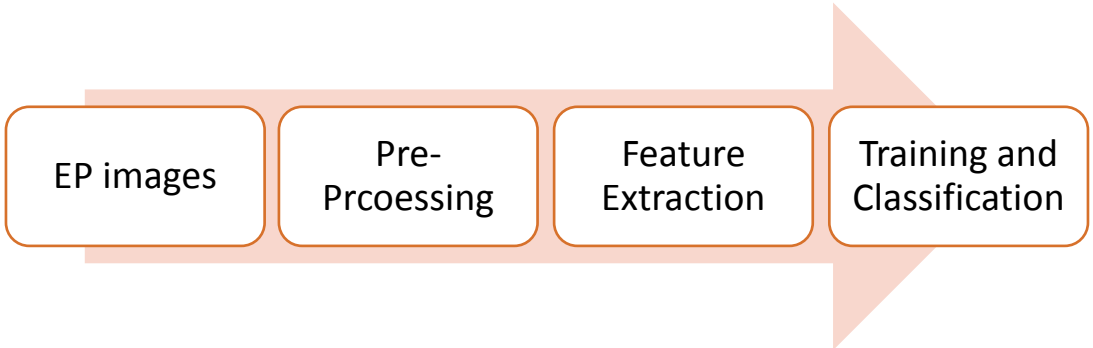


**Figure 2:** General block diagram of proposed methodology

Three separate steps can be used to describe the full process. The first step is to get the image dataset ready. In this process, photos from multiple sources are gathered for the analysis. The GDV image is typically affected by uniform light as a result of a number of problems, including a narrow lens, light reflection and diffusion instability, distortion, low contrast, camera inconsistencies, and device limits such the arrangement of ring-shaped light patterns. The pre-processing methods utilised in this methodology include resizing, smoothing, and colour change. Then, features are extracted from the preprocessed images. The preprocessed image is split into a training dataset and a test dataset before feature extraction. The model is created using a training set, and it is validated using a test set. The models are then balanced and tested using the training data. The basic goal of the extraction function is to choose the most significant data characteristics and present them in a lower-dimensional manner. The extracted image has the feature vector combination. Using Random Forest, the outcomes of the training and testing phases are compared for disease prediction.

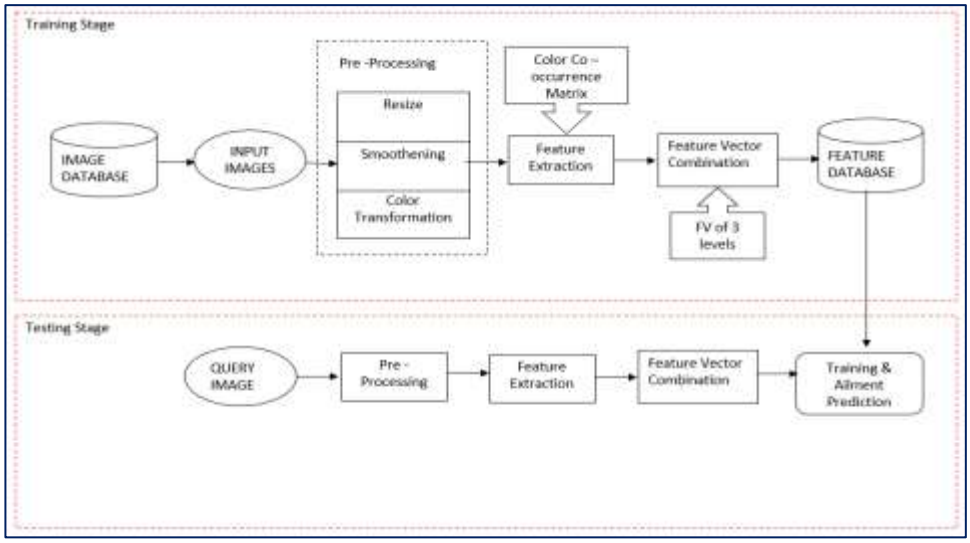


**Figure 3:** Block diagram of Training and Testing Stage of proposed system

**Pre-Processing**

Pre-processing is a term used to describe actions taken on images at their most basic level. Images of intensity are used as input and output. These recognisable images are of the same type as the original sensor data, with an intensity image often being represented by a matrix of brightness values for image function. The purpose of pre-processing is to increase certain image characteristics necessary for smoothing and to improve the image data by suppressing unintentional distortions. As a preprocessing technique for the examination of huge databases, resizing methods are used. The primary pre-processing approach in the suggested work is colour transformation. The goal of colour transformation is to identify the best colour space to utilise for the backdrop of the human image and the foreground of AURA separately. 16,777, `216 colours (256 * 256 * 256) are possible with plane colours at 24 bits per pixel (8 for each RGB value). A hue of 0 to 360 corresponds to blue, 120 to green, and 240 to red. Higher values signify more pure colours, and the saturation scale goes from 0 to 208. Higher numbers indicate brighter colours, and the value spans from around 0 to 512. The image's luminance or brightness values fall between [0, 100], where 0 denotes black and 100 denotes white. Colours get brighter as L rises'A' denotes how much of the image's tones are red or green. Red/magenta is represented by a strong positive value for 'A'. Green is represented by a significant negative 'A' value. Although 'A' does not have a specific range, values frequently fall between [-100, 100] and [-128, 127]. the image's proportion of yellow or blue tones. Yellow appears when the 'B' value is extremely positive. Blue is represented by a significant negative 'B' value. Although 'B' does not have a single range, values frequently fall between [-100, 100] and [-128, 127]. Additionally, the chrominance information is stored as two color-difference components (Cb and Cr), while the luminance information is stored as a single component (Y).

**A) Colour Co-occurance Matrix**

Feature extraction is the process of extracting an image's global or local features. Features are succinct, direct explanations of the data included

in the images. Three main mathematical operations make up the Colour Co-occurance Marix (CCM) procedure: (1) The image is converted from RGB to other colour representations such as grey [22], HSL and HSV [23], L*a*b* and XYZ [24], LCH and Luv [25] and CMY and CMYK [26], (2) Spatial Gray-Level Dependence Matrices (SGDMs) are calculated, producing one colour space model (CCM) for each colour space, and (3) fifteen Haralick textural features (TFs) are identified [27].

Angular Second Moment (ASM)

$$f_1 = \sum_{a=0}^{N_g-1} n^2 \sum_{b=0}^{N_g-1} P_{d,\theta}(a,b)^2$$

1) Contrast:

$$f_2 = \sum_{n=0}^{N_g-1} n^2 \sum_{\substack{a=1 \\ |a-b|=n}}^{N_g} \sum_{b=1}^{N_g} \{ p(a,b) \}^2$$

2) Entropy:

$$f_3 = -\sum_a \sum_b p(a,b) \log (p(a,b))$$

3) Variance:

$$f_4 = \sum_a \sum_b (a-\mu)^2 \; p(a,b)$$

4) Correlation:

$$f_5 = \sum_{a=1}^{N_g} \sum_{b=1}^{N_g} \frac{(a,b)p(a,b) - \mu_x \mu_y}{\sigma_x \sigma_y}$$

Where $\mu_x, \mu_y$, $\sigma_x$ *and* $\sigma_y$ are the means and standard deviations of the partial probability density function $p_x p_y$.

5) Inverse difference moment (IDM)

$$f_6 = \sum_{a=0}^{N_g-1} \sum_{b=0}^{N_g-1} \frac{1}{1+(a-b)^2} P_{d,\theta}(a,b)^2$$

6) Sum Average:

$$f_8 = \sum_{a=2}^{2N_g} i \, P_{x+y}(a)$$

$P_{x+y}(a)$ is the probability of co-occurrence matrix coordinates totalling *x*+*y* and *x* as well as *y* are the co-occurrence matrix coordinates of an entry.

7) Sum Variance:

$$f_9 = \sum_{a=2}^{2N_g} (a - f_8)^2 \, P_{x+y}(a)$$

8) Sum Entropy:

$$f_{10} = -\sum_{n=0}^{2N_g} P_{x+y}(a) log\{ P_{x+y}(a) \}$$

9) Correlation Information Measures 1:

$$f_{17} = \frac{HXY - HXY1}{max\{HX, HY\}}$$

10) Correlation Information Measures 2:

$$f_{18} = (1 - \exp[-2.0(HXY2 - HXY)])^2$$

$$HXY = -\sum_a \sum_b p(a,b) \log\big(p(a,b)\big)$$

Where HX and HY are the entropies of $P_x$ and $P_y$, respectively, and

$$HXY1 = -\sum_a \sum_b p(a,b) \log\{P_x(a)P_y(b)\}$$

$$HXY2 = -\sum_a \sum_b P_x(a)P_y(b) \log\{P_x(a)P_y(b)\}$$

11) Dissimilarity:

$$f_6 = \sum_a \sum_b |a-b| \; . \; p(a,b)$$

12) Maximum Probability

$$f_{14} = \underset{a,b}{MAX} \; p(a,b)$$

13) Energy:

$$f_1 = \sum_a \sum_b \{p(a,b)\}^2$$

The descriptions of each textural feature are as follows: Entropy gauges a gray-level distribution's unpredictability, whereas energy gauges the

quantity of repeated pairings; the local contrast image is measured by contrast; A pixel pair's local homogeneity is measured by homogeneity; In an image, the sum mean offers the average grey level, while the variance reflects how evenly distributed the grey levels are. a correlation between the two pixels in the pixel pair is provided by correlation; the pixel pair with the highest probability is the one that predominates in the image; The smoothness of the image is described by the IDM, while the clustering of pixels with comparable grey levels is measured by the cluster tendency. Statistical textural analysis is appropriate for an image of a biological thing.

**B) Automatic Ailment Prediction**

When used in machine learning, a classifier algorithm automatically groups or categorises data into one or more of a set of "classes." Machine learning algorithms are helpful for automating tasks that formerly needed manual labour. For businesses, they may dramatically reduce expenses while raising production. Here, we contrast the proposed strategy with SVM and RF classifier.

## III. Results and Discussion

A preprocessed image is subjected to a feature extraction method. From each plane in a single input image, 16 FV are calculated. FV1 is equivalent to (FV_R, FV_G, and FV_B) for an RGB image, and the feature vector has a size of 1x48 [(1x16, (1x16), (1x16)]. Figure 4 depicts the results of the colour transformation, where a) is the input image and 4 (b), (c), (d), and (e) are the results of the colour space transformation. For SVAM, RF, and Eada classifiers, the performance metrics of precision, recall, specificity, and accuracy were determined. Tables 1, 2, and 3 show the performance metrics for each colour space transformation using a different classifier, where Table 1 represents the SVM classifier, Table 2 represents the RF classifier, and Table 3 represents the Eada classifier, respectively. The values of the overall performance parameters for the various classifiers are shown in Table 4. The performance assessment graph for SVM, RF, and Eada is shown in Figure 5.

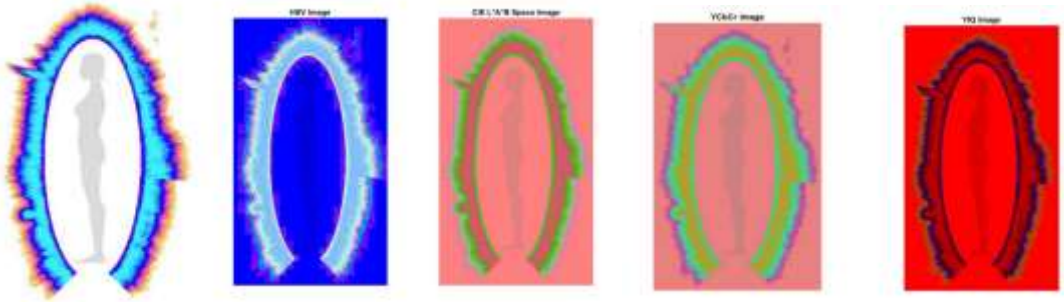

(a) (b) (c) (d) (e)

**Figure 4:** Output of Colour space Transformation
a) input image b) HSV image c) CIE space image d) YbCr image e) YIQ image

**Table 1:** Performance parameters value of SVM classifier for different Colour space Transformations

| SVM Evaluation | RGB | HSV | LAB | YCbCr | YIQ |
|---|---|---|---|---|---|
| **Precision** | 0.62 | 0.58 | 0.67 | 0.71 | 0.73 |
| **Recall** | 0.74 | 0.72 | 0.79 | 0.82 | 0.87 |
| **Specificity** | 0.11 | 0.1 | 0.21 | 0.28 | 0.37 |
| **Accuracy** | 0.53 | 0.49 | 0.6 | 0.65 | 0.7 |

**Table 2:** Performance parameters value of RF classifier for different Colour space Transformations

| Random Forest Evaluation | RGB | HSV | LAB | YCbCr | YIQ |
|---|---|---|---|---|---|
| **Precision** | 0.67 | 0.62 | 0.71 | 0.76 | 0.78 |
| **Recall** | 0.79 | 0.78 | 0.84 | 0.85 | 0.9 |
| **Specificity** | 0.21 | 0.19 | 0.32 | 0.35 | 0.44 |
| **Accuracy** | 0.6 | 0.56 | 0.67 | 0.7 | 0.75 |

**Table 3:** Performance parameters value of Eada classifier for different Colour space Transformations

| Ensembled Adaboost Evaluation | RGB | HSV | LAB | YCbCr | YIQ |
|---|---|---|---|---|---|
| **Precision** | 0.78 | 0.71 | 0.8 | 0.8 | 0.87 |

| | | | | | |
|---|---|---|---|---|---|
| **Recall** | 0.81 | 0.76 | 0.86 | 0.84 | 0.98 |
| **Specificity** | 0.29 | 0.13 | 0.4 | 0.36 | 0.65 |
| **Accuracy** | 0.68 | 0.6 | 0.74 | 0.72 | 0.88 |

**Table 1:** Overall performance parameters value for different classifiers

| Classifier Evaluation | SVM | RF | Eada |
|---|---|---|---|
| **Precision** | 0.73 | 0.78 | **0.87** |
| **Recall** | 0.87 | 0.9 | **0.98** |
| **Specificity** | 0.37 | 0.44 | **0.65** |
| **Accuracy** | 0.7 | 0.75 | **0.88** |

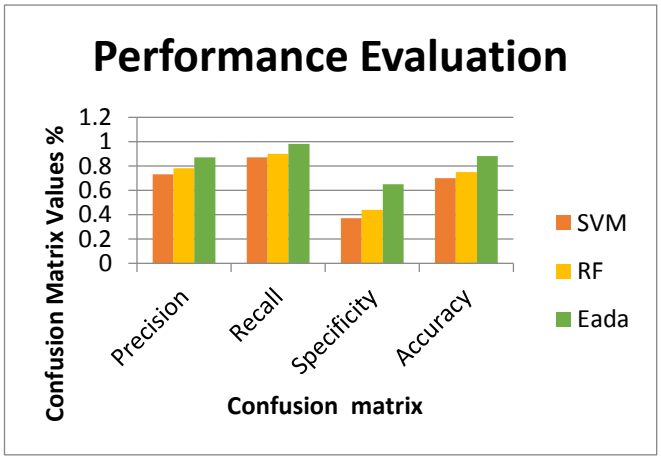


**Figure 5:** Performance Evaluation graph for SVM, RF and Eada.

We can see from the performance characteristics shown in the tables and figures that the accuracy of the SVM is 70%, that of the RF is 75%, and that of the suggested approach Eada classifier is 88%. Comparing the suggested approach to the existing algorithm, it was found to be superior.

**Conclusion and Future Scope**

The detection of diseases is the focus of the biometrics subfield known as medical biometrics. AURA pictures from the GDV will be used to identify the variances. The present needs of medical biometrics to recognise a disease at an early stage of development, which will manifest as a rise in entropy and divergence from the normal functional state, may be satisfied by GDV. For colour information in this work, colour spaces like HSV, L*a*b, YCbCr, etc. can be utilised. For more thorough feature extraction, CCM may be employed with different direction and distance. Various feature combinations and well-known classification methods were employed to introduce the prediction model. With an accuracy score of 88%, the Ensembled Adaboost was shown to be the most accurate in predicting illnesses. Future research must focus on developing more sophisticated ML algorithms to improve the accuracy of illness prediction. Additionally, several segmentation techniques may be used with ROI detection to determine which organ or region is most likely to be affected. Additionally, databases on various demographics need to be extended so that we can compute the energy and balance. Finally, to improve the performance of the learning models, more pertinent feature selection techniques should be applied.

References

1. Beverly Rubik, “Measurement of the Human Biofield and Other Energetic Instruments”, Energetics and Spirituality by Lyn Free man, 2008.
2. Hammerschlag R, Levin M, McCraty R, Bat N, Ives JA, Lutgendorf SK, Oschman JL. Biofield Physiology: A Framework for an Emerging Discipline. Glob Adv Health Med. 2015 Nov;4(Suppl):35-41.
3. https://www.speakingtree.in/allslides/ the-scientific-evidence-of-human-aura
4. Chhabra, Gunjan & Prasad, Ajay & Marriboyina, Venkatadri. (2019). Comparison and performance evaluation of human bio-field visualization algorithm. Archives of Physiology and Biochemistry.
5. International Conference on Medical Biometrics. 2010, http://www4. comp.polyu. edu.hk/~icbd/

6. Korotkov, KG. Human energy field study with GDV bioelectrography. Fair Lawn, New Jersey: Backbone Publishing; 2002.
7. Korotkov K, Williams B, Wisneski LA. Assessing biophysical energy transfer mechanisms in living systems: the basis of life processes. J Altern Complement Med. 2004; 10:49–57.
8. Korotkov KG, Matravers P, Orlov DV, Williams BO. Application of electrophoton capture (EPC) analysis based on gas discharge visualization (GDV) technique in medicine: a systematic review. J Altern Complement Med. 2010; 16:13–25.
9. Kostyuk N, Cole P, Meghanathan N, Isokpehi RD, Cohly HH. Gas discharge visualization: an imaging and modeling tool for medical biometrics. Int J Biomed Imaging.
10. H. Cohly, N. Kostyuk, R. Isokpehi, and R. Rajnarayanan, "Bio-electrographic method for preventive health care," in Proceedings of the 1st IEEE Annual Bioscience and Biotechnology Conference, 2009.
11. Yin M, Panigrahi S 2004 Image processing techniques for internal texture evaluation of French fries Appl. Eng. Agric. 206 803-811.
12. Shearer S A 1986 Plant identification using colour co-occurrence matrices derived from digitized images PhD Dissertation Department of Agricultural Engineering Ohio State University Columbus Ohio USA.
13. Philipp I, Rath T 2002 Improving plant discrimination in image processing by use of different colour space transformations Comput. Electron. Agric. 35 1-15
14. Hendrawan Y, Murase H 2010 Neural-Genetic Algorithm as feature selection technique for determining sunagoke moss water content Eng. Agric. Environ. Food (EAEF) J. 3 1 25-31
15. Hendrawan Y, Murase H 2011 Non-destructive sensing for determining Sunagoke moss water content: Bio-inspired approaches Agric. Eng. Int.: CIGR Journal 15 64 131.
16. Hendrawan Y, Murase H 2011 Bio-inspired feature selection to select informative image features for determining water content of cultured Sunagoke moss Expert Syst. Appl. 381 4321-14335.
17. Hendrawan Y, Murase H 2011 Neural-intelligent water drops algorithm to select relevant textural features for developing precision irrigation system using machine vision Comput. Electron. Agric. 772 214-228.
18. Hendrawan Y, Murase H 2011 Neural-discrete hungry roach infestation optimization to select informative textural features for determining water content of cultured Sunagoke moss Environ. Control Biol. 491 1-21.
19. Hendrawan Y, Al Riza D F 2016 Machine vision optimization using Nature –inspired algorithms to model Sunagoke moss water status Int. J. Adv. Sci. Eng. Inform. Technol. 6 2088-5334.
20. Shulginov.A.; Stadnik.O.S. "Recognition and Classification of Plasma Clots of Bioelectograms" 2018 Global Smart Industry Conference (Glosic), 978-1-5386-7386
21. Gunjan Chhabra, Ajay Prasad, Venkatadrimarriboyina "Future Trends of Artificial Intelligence In Humanbiofield" International Journal Of Innovative Technology And Exploring Engineering (Ijitee) Issn: 2278- 3075, Volume-8 Issue-10, August 2019
22. Rotterman Y, Porat M 2006 Colour image coding using regional correlation of primary colours Image Vision Comput. 25 637-651.
23. Angulo J, Serra J 2007 Modelling and segmentation of colour images in polar representations Image Vision Comput. 25 475-495
24. Leon K, Mery D, Pedreschi F, Leon F 2006 Colour measurement in L*a*b* units from RGB digital images Food Res. Int. 39 1084-1091
25. Kim M C 2008 Comparative colour gamut analysis of xvYCC standard Displays 29 376-385
26. Palm C 2004 Colour texture classification by integrative Co-occurrence matrices Pattern Recogn. 37 965-976.
27. Hendrawan Y, Murase H 2011 Non-destructive sensing for determining Sunagoke moss water content: Bio-inspired approaches Agric. Eng. Int.: CIGR Journal 15 64 131.